11th Annual CFD Symposium
11th – 12th August 2009, Bangalore

COMPUTATION OF TURBULENT JETS IN ANNULAR COUNTER-FLOW

M. Sivapragasam[1], S. Ramamurthy[2], M. D. Deshpande[3], S. N. Sridhara[4]

Abstract

A turbulent jet issuing into a uniform counter-flow has many engineering applications in various mixing and combustion processes. In this paper the flow field of a turbulent jet issuing into a uniform annular confined counter-flow stream was computationally investigated. The results are presented in terms of the velocity field, pertinent velocity and length scales, and turbulence characteristics and compared with available experimental data.

Keywords

turbulent jet, computational fluid dynamics, turbulence modelling, centreline velocity decay, turbulence intensity.

Introduction

A turbulent jet is a basic free shear flow and has received extensive research attention (see, for example, Pope [1]). However, in many engineering applications the jet does not issue into a quiescent stream but interacts with an external stream. This interaction can be classified as co-flow, cross-flow or counter-flow depending on the direction of interaction between the jet and the external stream. Of these interactions, the jet in counter-flow is least investigated because of the extreme theoretical and experimental difficulties associated with the reverse flow phenomenon and marked instability of the flow. Interestingly, these flow characteristics which are responsible for the complexity of the flow also contribute to enhanced mixing efficiency thus rendering the jet in counter-flow configuration suitable for various mixing and combustion processes.

The earliest study of a turbulent jet in counter-flow was reported by Arendt *et al.* [2]. Some early Russian workers investigated the flow field of a jet in counter-flow, most notably Sekundov [3]. Beltaos and Rajaratnam [4] presented their results based on their experiments, dimensional analysis, and semi-empirical relations. More recently two research groups, one at the Technical University of Berlin (Yoda and Fiedler [5], Bernero [6], Bernero and Fiedler [7]), and the other at the University of Hong Kong (Lam and Chan [8, 9], Chan and Lam [10]), and a collaborative work between these groups (Chan *et al.* [11]), had published experimental results of the counter-flow jet flow field. These groups' work had focused on the velocity and concentration fields of a jet issuing into an infinite counter-flow.

The present study pertains to the computational investigation of the flow field of a turbulent jet issuing into an annular confined uniform counter-flow. A series of parametric computations were performed for different annular-to-jet diameter ratios and for various jet-to-counter-flow velocity ratios. All time-averaged calculations were performed with a standard k-ε turbulence model using the FLUENT flow solver. The results are presented in terms of the streamline pattern, the velocity profiles in the jet, the decay of velocity along the jet centreline and pertinent velocity and length scale parameters, among others. Comparisons with available experimental data are made wherever possible.

[1] Research Scholar, Centre for Fluid Flow and Energy Systems Research, M. S. Ramaiah School of Advanced Studies, Bangalore – 560 054. E-mail: msp@msrsas.org
[2] Deputy Head, Propulsion Division, National Aerospace Laboratories, Bangalore – 560 017.
[3] Head, Research, M. S. Ramaiah School of Advanced Studies, Bangalore – 560 054.
[4] Head, Department of Mechanical and Automotive Engineering, M. S. Ramaiah School of Advanced Studies, Bangalore – 560 054.

Description of the Flow Field

A schematic illustration of the flow field is depicted in Fig. 1. Consider a steady, incompressible turbulent jet of velocity u_j issuing from a nozzle of diameter d into steady uniform stream of velocity u_0 ($u_j > u_0$) confined within a duct of diameter D. The direction of freestream velocity is opposite to that of the jet. The jet penetrates into the counter-flow stream up to a distance l_p, then interacts with the freestream and deflects backwards. The jet penetration and backward deflection is a peculiar characteristic of the jet in counter-flow configuration which is not found in free jets or jets in co- or cross-flow.

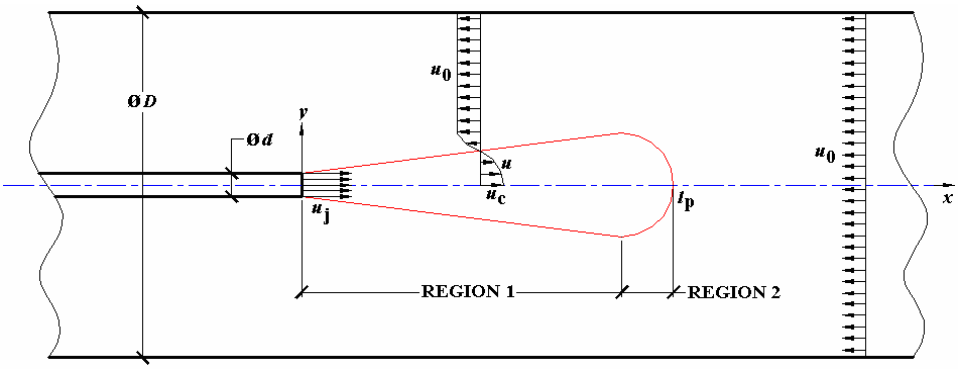

Fig. 1 Schematic description of the flow field

Following convention the jet flow field can be divided into two distinct regions along its axial length. Region 1 at the exit of the nozzle is where the jet flow dominates and the jet at least qualitatively behaves like a free jet. The flow rate and the jet thickness increases with distance from the nozzle and subtend an angle arc tan 0.22 (Sekundov [3]) from the jet axis. The static pressure is approximately constant in this region. The counter-flow prevails in region 2 and the static pressure is not constant here. The jet is acutely opposed by the counter-flow and is characterised by a highly turbulent field of flow.

Computational Procedure

The governing equations of mass and momentum conservation for a turbulent flow field namely, the Reynolds-averaged Navier-Stokes equations,

$$\frac{\partial \bar{u}_i}{\partial x_i} = 0$$

$$\frac{\partial \bar{u}_i}{\partial t} + \frac{\partial \bar{u}_i \bar{u}_j}{\partial x_j} = -\frac{1}{\rho}\frac{\partial \bar{p}}{\partial x_i} + \frac{\partial}{\partial x_i}\left[\nu\left(\frac{\partial \bar{u}_i}{\partial x_j} + \frac{\partial \bar{u}_j}{\partial x_i}\right) - \overline{u_i' u_j'}\right]$$

are solved numerically using the FLUENT (Version 6.3) flow solver. Here, $-\overline{u_i' u_j'}$ are the Reynolds stresses and are modelled by the Boussinesq hypothesis relating these stresses to the gradients in mean velocity.

The time-averaged computations were performed for a range of annular-to-jet diameter ratios (D/d) from 5 to 30 and jet-to-counter-flow velocity ratios (u_j/u_0) ranging from 2 to 20. An axisymmetric structured grid was devised for the computations. A cylindrical coordinate system was chosen and its origin was fixed at the jet exit. The counter-flow stream inlet was placed at a distance 50 d ahead of the jet exit and the flow domain outlet was at 50 d behind the jet exit. The computational domain for the numerical solution consisted of 45,000 (500 axial x 90 radial) cells for D/d = 5; 95,000 (500 x 190) for D/d = 10; 145,000 (500 x 290) for D/d = 15; and 354,000 (600 x 590) for D/d = 30. The number of computational cells was chosen after a careful grid independence study.

The velocity inlet boundary condition was specified at the counter-flow stream inlet and the jet inlet. The exit static pressure was specified at the outlet boundary at x = -50 d. On the walls bounding the flow domain the no-slip boundary condition was imposed.

All computations were performed by a standard k-ε turbulence closure model (Launder and Spalding [13]). This model calculates the turbulence viscosity as,

$$\nu_t = C_\mu \frac{k^2}{\varepsilon}$$

where C_μ is a constant. The model constants are assigned the following values:

$$C_{1\varepsilon} = 1.44\,,\ C_{2\varepsilon} = 1.92\,,\ C_\mu = 0.09\,,\ \sigma_k = 1.0\,,\ \sigma_\varepsilon = 1.3\,.$$

The segregated-implicit solver which sequentially solves the mass and momentum conservation equations was activated to obtain the converged solutions. The first-order upwind scheme was employed to discretise the governing equations. The pressure-velocity coupling was achieved by the SIMPLE algorithm. A convergence criterion of 10^{-5} was set on the continuity equation. All calculations were carried out in double-precision arithmetic.

Results and Discussion

Velocity Field

The normalised stream function contour is shown in Fig. 2 for a diameter ratio of 10 and a velocity ratio of 20. The jet originating from the nozzle and penetrating into the counter-flow stream can be seen in this figure. The recirculation region is also observed in this figure.

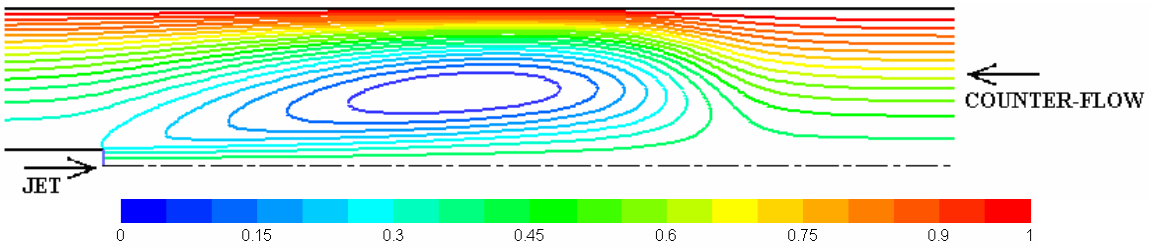

Fig. 2 Contours of normalised stream function (ψ/ψ_{max}) (D/d=10; u_j/u_0=20)

The axial velocity distribution in the radial direction at various streamwise locations along the jet can be plotted using the self-similarity hypothesis. Beltaos and Rajaratnam [4] gave the following expression for the self-similarity of the velocity profiles in the jet in infinite counter-flow

$$\frac{u - u_0}{u_c - u_0} = \left[1 + 0.59\left(\frac{y}{b}\right)^2\right]^{-3/2}.$$

In the above relation the local excess velocity ($u - u_0$) is normalised by the excess velocity at the jet centreline ($u_c - u_0$); the radial coordinate is normalised by the local jet width b. The jet width is defined as the radial distance where the local excess velocity equals one-half of the centreline excess velocity. It is to be noted that self-similarity of velocity profiles are to be expected only in region after the development of the jet and before its backward deflection.

The velocity profiles from the computational analysis are plotted in Fig. 3 for different diameter ratios at the highest velocity ratio of 20 considered in this parametric analysis. It can be seen that the computational results compare well with the analytical curve. The analytical curve is valid for infinite counter-flow and the computational results match better for the highest diameter ratio of 30 considered here.

The self-similar velocity distribution for a free jet is also plotted in Fig. 3 for reference. It serves well to note that the velocity distribution compares well with that of a free jet near the axis till about y/b is unity. The inner region near the axis of the jet is free from the influence of the counter-flow and behaves much like a free jet. Away from the jet axis the counter-flow influences the jet and departure from the free jet behaviour is observed. It is clear that the jet in counter-flow spreads faster than a jet in quiescent ambient.

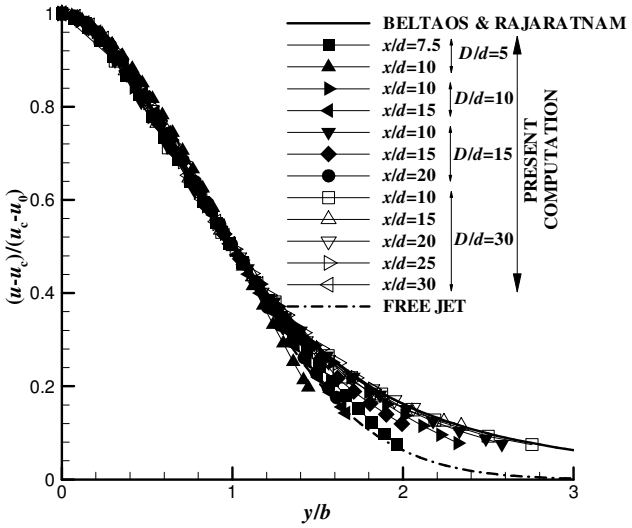

Fig. 3 Self-similar velocity profiles (u_j/u_0=20)

Penetration Length

A number of results are available on the penetration of the jet into the counter-flowing stream. Most of these investigations considered the counter-flow to be infinite and arrived at a linear relation between the penetration length and the jet-to-counter-flow velocity ratio. This linear relation is of the form,

$$\frac{l_\mathrm{p}}{d} = c' \frac{u_\mathrm{j}}{u_0}$$

In spite of consistent results from various sources the value of the linearity constant *c*' varies in the range from 2.4 to 2.9. Bernero [6] suggested a reference value of 2.7 can be used for practical purposes.

The presence of the external bounding walls can cause the breakdown of penetration length-velocity ratio linear relationship. In fact, the effect of confinement is to reduce the penetration length of the jet compared to the unconfined case.

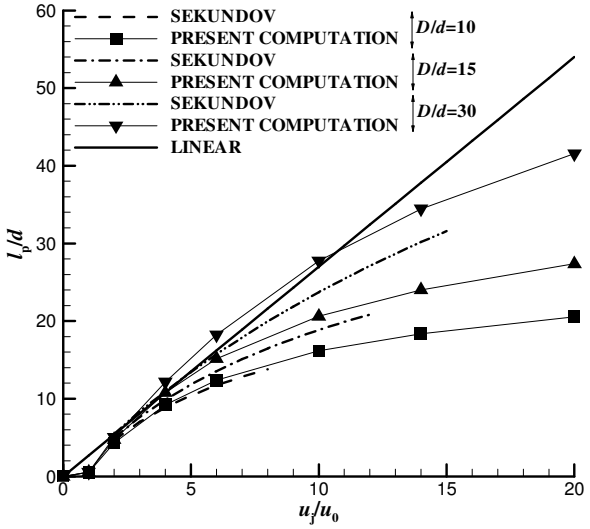

Fig. 4 Variation of penetration length with jet-to-counter-flow velocity ratio

The results from the present computational analysis are presented in Fig. 4. Also plotted in the same figure are the results from the analysis of Sekundov [3]. This integral method assumed linear velocity profiles for integration and resulted in a complicated expression for the penetration length. A mixing length hypothesis was employed and the analysis was limited by the boundary-layer assumptions. The

experimental investigations of Morgan *et al*. [13] and the computational and experimental results of Majumdar and Bhaduri [14] also confirm the non-linear trend between the penetration length and velocity ratio.

Jet Width

Again using dimensional arguments Beltaos and Rajaratnam [4] gave an empirical relation for the length scale which is the jet half-width *b*. Their expression was,

$$\frac{b}{l_\mathrm{p}} = 0.2 \frac{x/l_\mathrm{p}}{\sqrt{\left(\frac{2.24}{x/l_\mathrm{p}}\right)^{2/3} - 1}}.$$

The results from computational analysis are shown in Fig. 5 along with the empirical equation. It might be noted that the effect of confinement of the annular duct is to reduce the width of the jet. However, as the diameter ratio increases the trend is towards the Beltaos and Rajaratnam curve.

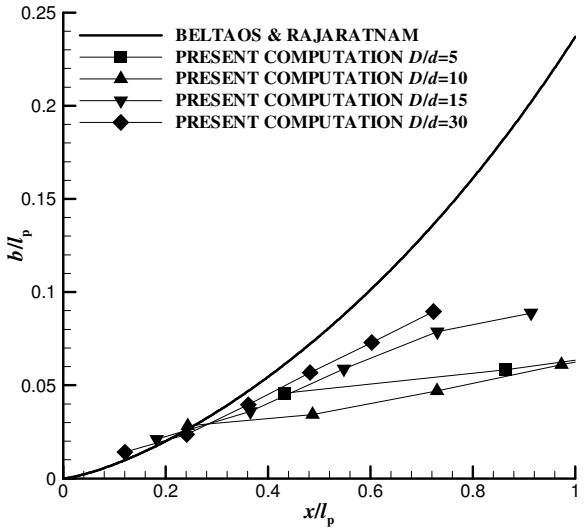

Fig. 5 Jet width growth along the jet

Centreline Velocity Decay

The axial velocity decay along the jet centreline follows an x^{-1} law very much alike the free jet situation. An exceptional change from the free jet behaviour is observed in region 2 (see Fig. 1) where the jet and the counter-flow interaction are intense. Beltaos and Rajaratnam [4] employed a hyperbolic decay curve and assumed a model constant value of 5.83. Yoda and Fiedler [5] from their flow visualisation experiments proposed the following simple model based on the superposition of a jet and a uniform counter-flow

$$\frac{u_\mathrm{c}}{u_\mathrm{j}} = \frac{5.8}{x/d}.$$

Chan and Lam [10] proposed an analytical model supported by their experimental observations. They hypothesised an advection effect of the counter-flow on the jet issuing from the nozzle through a Lagrangian formulation. This model is given as,

$$u_\mathrm{c} = \frac{u_\mathrm{j} l_\mathrm{m}}{x^*} + u_0 \log\left(\frac{u_\mathrm{j} l_\mathrm{m}}{x^*} - u_0\right) - u_0 \log\left(u_\mathrm{j} - u_0\right) \quad ; \quad x^* > l_\mathrm{m}.$$

The axial coordinate x should start from an origin shifted by a distance d_v, which is given as, $d_v = \frac{u_0}{u_0 + u_j} 6.2\,d$. (The length of the potential core of the jet in stagnant ambient is 6.2d). Now, $x^* = x + d_v$. The potential core length for a jet in counter-flow l_m is given by, $l_m = 6.2\,d\,\frac{u_j}{u_j + u_0}$.

Bernero [6] extended Yoda and Fiedler's [5] idea of a jet and counter-flow superposition and suggested the following model

$$\left(\frac{u_c - u_0}{u_j}\right)\frac{l_p}{d} = \left(\frac{c}{2}\right)\frac{1+\sqrt{1-x/l_p}}{x/l_p}\,.$$

He assumed c = 5.83 as suggested by Beltaos and Rajaratnam [4].

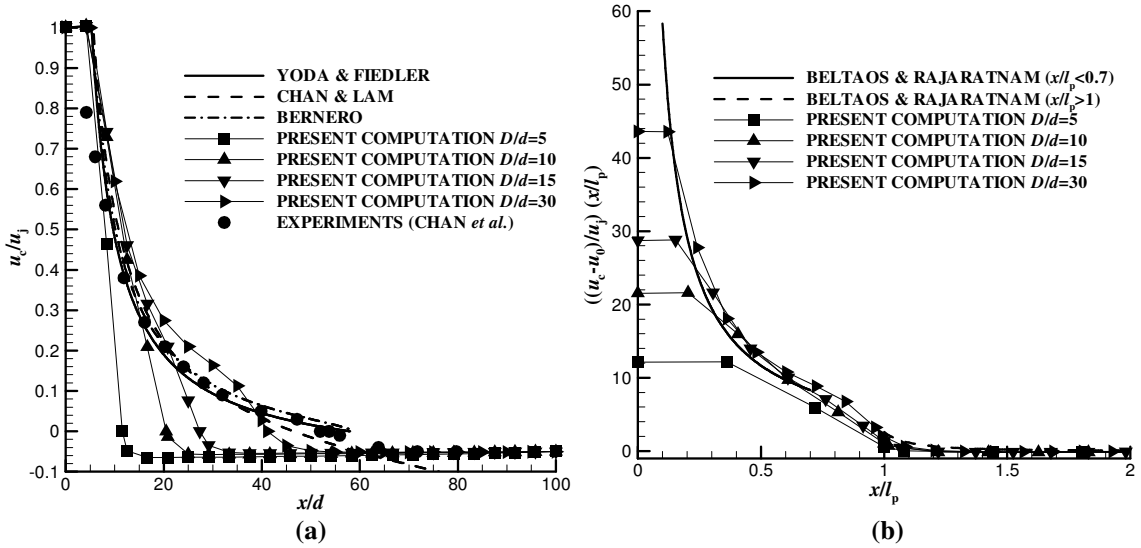

(a) **(b)**

Fig. 6 Centreline velocity decay (u_j/u_0=20)

The results from the present computational analysis are indicated in Fig. 6a along with the various models described in the previous paragraphs. The effect of confining duct is obviously seen in this figure. The annular confining ducts negate the validity of the analytical proposed models. However, good comparison is obtained at a large diameter ratio of 30 from the present computational study. More importantly, the comparison with the experiments of Chan *et al*. [11] is very encouraging.

The discrepancy between the present computation and experiments may be due to the extreme difficulty in both modelling and measuring the flow field interaction between the jet and the counter-flow beginning at approximately 70% of the penetration length.

An alternate scale for the centreline velocity proposed by Beltaos and Rajaratnam [4] is useful in collapsing the computational data presented in Fig. 6a. The centreline excess velocity ($u_c - u_0$) normalised by jet velocity (u_j) and multiplied by the non-dimensional penetration length (l_p/d) is chosen as the ordinate. The relation is,

$$\left(\frac{u_c - u_0}{u_j}\right)\frac{l_p}{d} = \frac{5.83}{x/l_p} \text{ for } x/l_p \le 0.7\,, \text{ and } \left(\frac{u_c - u_0}{u_j}\right)\frac{l_p}{d} = \frac{0.104}{\left[\left(\frac{x/l_p - 0.8}{l_p}\right)\right]^2} \text{ for } x/l_p \ge 1\,.$$

They indicated a smooth curve should join these two regimes.

The results are indicated in Fig. 6b. As noted earlier the centreline velocity decay curve for different diameter ratios collapse into a single curve.

Centreline Turbulence Intensity

The turbulence intensity is a measure of the turbulent velocity field fluctuations and is defined as the ratio of the root-mean-square of the velocity fluctuations to mean velocity (Schlichting and Gersten [15])

$$I = \frac{\sqrt{\overline{u'^2}}}{\overline{u}}.$$

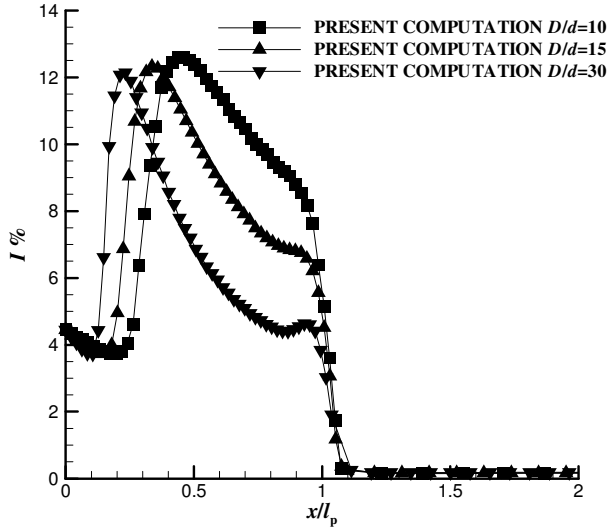

Fig. 7 Centreline turbulence intensity (u_j/u_0=20)

The downstream variation of centreline turbulence intensity is plotted in Fig. 7 for various diameter ratios. It is observed that two distinct peaks appear; they are also found to be independent of the velocity ratio. This observation is consistent with the experimental results of Tsunoda and Saruta [16]. The first peak is associated with the basic instability of the jet and the second peak near the maximum penetration length is due to the backward deflection of the jet by the opposing counter-flow resulting in intense turbulent activity. This second peak is a peculiar characteristic of this particular flow configuration. After the second peak the turbulence intensity decays to the counter-flow free stream value.

Conclusions

A turbulent jet issuing into a uniform annular counter-flow stream was computationally investigated. A series of parametric numerical studies was done for different annular-to-jet diameter ratios and various jet-to-counter-flow velocity ratios. It was observed that the jet in confined counter-flow behaves differently from the jet in infinite counter-flow. As expected the penetration length of the jet is reduced and the linear relationship between the velocity ratio and penetration length ceases to be valid. The computed centreline velocity decay compares well with the analytical model for the highest diameter ratio considered in the present computation. The peculiar two peaks in the computed centreline turbulence intensity are also consistent with the experimental observations.

Nomenclature

$C_{1\varepsilon}$, $C_{2\varepsilon}$, C_μ	model constants (in standard k- ε turbulence model)
D	annular diameter
I	turbulence intensity
b	jet half-width
c	constant (c=5.83 in Beltaos and Rajaratnam [4])
c'	constant (c'=2.7 suggested by Bernero [6])
d	jet diameter

k	turbulence kinetic energy
l_p	penetration length
u	velocity
u'	fluctuating velocity
x	axial coordinate
y	radial coordinate
Greek Symbols	
ε	turbulence dissipation rate
ν_t	turbulence viscosity
σ_k, σ_ε	model constants
Subscripts	
c	centreline
j	jet
0	counter-flow stream

References

[1] Pope, S. B., 2000, Turbulent Flows, Cambridge University Press, Cambridge, U. K.

[2] Arendt, J., Babcock, H. A., and Schuster, J., 1956, "Penetration of a Jet into a Counterflow," ASCE J. Hydr. Div., 82, pp. 1038-8-11.

[3] Sekundov, A. N., 1969, "The Propagation of a Turbulent Jet in an Opposing Stream," Turbulent Jets of Air, Plasma and Real Gas, G. N. Abramovich, ed., Consultants Bureau, N. Y., pp. 99-109.

[4] Beltaos, S., and Rajaratnam, N., 1973, "Circular Turbulent Jet in an Opposing Infinite Stream," Proc. 1st Canadian Hydrotechnical Conf., Edmonton, pp. 220-237.

[5] Yoda, M., and Fiedler, H. E., 1996, "The Round Jet in a Uniform Counterflow: Flow Visualization and Mean Concentration Measurements," Exp. Fluids, 21, pp. 427-436.

[6] Bernero, S., 2000, "A Turbulent Jet in Counterflow," Ph. D. Thesis, Technical University of Berlin, Berlin.

[7] Bernero, S., and Fiedler, H. E., 2000, "Application of Particle Image Velocimetry and Proper Orthogonal Decomposition to the Study of a Jet in a Counterflow," Exp. Fluids, (Suppl.), pp. S274-S281.

[8] Lam, K. M., and Chan, C. H. C., 1995, "Investigation of Turbulent Jets issuing into a Counterflowing Stream using Digital Image Processing," Exp. Fluids, 18, pp. 210-212.

[9] Lam, K. M., and Chan, C. H. C., 1997, "Round Jet in Ambient Counterflowing Stream," ASCE J. Hydraul. Eng., 123, pp. 895-903.

[10] Chan, C. H. C., and Lam, K. M., 1998, "Centreline Velocity Decay of a Circular Jet in a Counterflowing Stream," Phys. Fluids, 10, pp. 637-644.

[11] Chan, C. H. C., Lam, K. M., and Bernero, S., 1999, "On the Penetration of a Round Jet into a Counterflow at different Velocity Ratios," Environmental Hydraulics, J. H. W. Lee, A. W. Jayawardena, and Z. Y. Yang, eds., Balkema, Rotterdam, pp. 229-234.

[12] Launder, B. E., and Spalding, D. B., 1972, Lectures in Mathematical Models of Turbulence, Academic Press, London.

[13] Morgan, W. D., Brinkworth, B. J., and Evans, G. V., 1976, "Upstream Penetration of an Enclosed Counterflowing Jet," Ind. Eng. Chem. Fundam., 15, pp. 125-127.

[14] Majumdar, S., and Bhaduri, D. 1981, "On Recirculating Flow in an Opposed Jet Flame Holder," Appl. Math. Modelling, 5, pp. 179-184.

[15] Schlichting, H., and Gersten, K., 2001, Boundary-Layer Theory, Eighth Edition, Springer, New Delhi.

[16] Tsunoda, H., and Saruta, M., 2003, "Planar Laser-Induced Fluorescence Study on the Diffusion Field of a Round Jet in a Uniform Counter-flow," J. Turbulence, 4, Art. No. N13.